

# Activation of cyclic electron flow by hydrogen peroxide in vivo

Deserah D. Strand<sup>a,b</sup>, Aaron K. Livingston<sup>c,d,1</sup>, Mio Satoh-Cruz<sup>a</sup>, John E. Froehlich<sup>a,e</sup>, Veronica G. Maurino<sup>f</sup>, and David M. Kramer<sup>a,b,e,2</sup>

<sup>a</sup>Plant Research Laboratory and Departments of <sup>b</sup>Plant Biology and <sup>c</sup>Biochemistry and Molecular Biology, Michigan State University, East Lansing, MI 48824; <sup>d</sup>School of Molecular Biosciences and <sup>e</sup>Institute for Biological Chemistry, Washington State University, Pullman, WA 99164; and <sup>f</sup>Institute of Developmental and Molecular Biology of Plants, Plant Molecular Physiology and Biotechnology Group, Heinrich-Heine-Universität, Cluster of Excellence on Plant Sciences (CEPLAS), 40225 Düsseldorf, Germany

Edited by Bob B. Buchanan, University of California, Berkeley, CA, and approved March 9, 2015 (received for review September 23, 2014)

Cyclic electron flow (CEF) around photosystem I is thought to balance the ATP/NADPH energy budget of photosynthesis, requiring that its rate be finely regulated. The mechanisms of this regulation are not well understood. We observed that mutants that exhibited constitutively high rates of CEF also showed elevated production of H<sub>2</sub>O<sub>2</sub>. We thus tested the hypothesis that CEF can be activated by H<sub>2</sub>O<sub>2</sub> in vivo. CEF was strongly increased by H<sub>2</sub>O<sub>2</sub> both by infiltration or in situ production by chloroplast-localized glycolate oxidase, implying that H<sub>2</sub>O<sub>2</sub> can activate CEF either directly by redox modulation of key enzymes, or indirectly by affecting other photosynthetic processes. CEF appeared with a half time of about 20 min after exposure to H<sub>2</sub>O<sub>2</sub>, suggesting activation of previously expressed CEF-related machinery. H<sub>2</sub>O<sub>2</sub>-dependent CEF was not sensitive to antimycin A or loss of PGR5, indicating that increased CEF probably does not involve the PGR5-PGRL1 associated pathway. In contrast, the rise in CEF was not observed in a mutant deficient in the chloroplast NADPH: PQ reductase (NDH), supporting the involvement of this complex in CEF activated by H<sub>2</sub>O<sub>2</sub>. We propose that H<sub>2</sub>O<sub>2</sub> is a missing link between environmental stress, metabolism, and redox regulation of CEF in higher plants.

cyclic electron flow | photosynthesis | reactive oxygen species | stress | hydrogen peroxide

In oxygenic photosynthesis, linear electron flow (LEF) is the process by which light energy is captured to drive the extraction of electrons and protons from water and transfer them through a system of electron carriers to reduce NADPH. LEF is coupled to proton translocation into the thylakoid lumen, generating an electrochemical gradient of protons ( $\Delta\mu_{H^+}$ ) or proton motive force (*pmf*). The *pmf* drives the synthesis of ATP to power the reactions of the Calvin–Benson–Bassham (CBB) cycle and other essential metabolic processes in the chloroplast. The *pmf* is also a key regulator of photosynthesis in that it activates the photo-protective *q<sub>E</sub>* response to dissipate excess light energy and down-regulates electron transfer by controlling the rate of oxidation of plastoquinol at the cytochrome *b<sub>6</sub>f* complex (*b<sub>6</sub>f*), thus preventing the buildup of reduced intermediates (1, 2).

LEF results in the transfer or deposition into the lumen of three protons for each electron transferred through PSII, plastoquinone (PQ), *b<sub>6</sub>f*, plastocyanin, and photosystem I (PSI) to ferredoxin (Fd). The synthesis of one ATP is thought to require the passage of 4.67 protons through the ATP synthase, so that LEF should produce a ratio of ATP/NADPH of about 1.33; this ratio is too low to sustain the CBB cycle or supply ATP required for translation, protein transport, or other ATP-dependent processes (3). In addition, the relative demands for ATP and NADPH can change dramatically depending on environmental, developmental, and other factors, leading to rapid energy imbalances that require dynamical regulation of ATP/NADPH balance.

Several alternative electron flow pathways in the chloroplast have been proposed to augment ATP production, thus balancing the ATP/NADPH budget of the chloroplast (2, 3). Perhaps the

most important and complicated of these pathways is cyclic electron flow around photosystem I (CEF), in which electron flow from the acceptor side of PSI is shunted back into the PQ pool, generating additional *pmf* that can power ATP production without net NADPH production. There are several proposed CEF pathways that may operate under different conditions or in different species (reviewed in refs. 2 and 3). In higher-plant chloroplasts, the most studied routes of CEF are the antimycin A-sensitive pathway, which involves a complex of two CEF-related proteins, PGR5 (Proton Gradient Regulation 5) and PGRL1 (PGR5-like 1), directly reducing the quinone pool (4–7), the respiratory complex I analog, the NADPH dehydrogenase (NDH) complex (8–10), which oxidizes Fd or NAD(P)H to reduce plastoquinone (8, 11), and through the *Q<sub>i</sub>* site of *b<sub>6</sub>f* (12, 13). Different CEF mechanisms seem to operate in other species. In *Chlamydomonas*, for example, CEF seems to be conducted by a supercomplex of PSI, *b<sub>6</sub>f*, and the PGRL1 protein (14, 15), and the involvement of PGR5 has recently been described as important for CEF under hypoxia (16, 17).

Regardless of the mechanism of CEF, the overall process must be well regulated to properly balance the production of ATP to match the demands of metabolism. The mechanism of this regulation is not known, but many general models have been proposed. Perhaps the most widely cited regulatory model is the antenna state transition, which was previously shown to be correlated with activation of CEF in *Chlamydomonas reinhardtii* (14, 18) and favor the formation of the PSI–*b<sub>6</sub>f* supercomplex (14). However, it was recently shown that state transitions are not required for CEF activation, supporting models that include redox control (15–17, 19–22). Other possible regulatory mechanisms include sensing of ATP/ADP ratios (23, 24), the redox status of NAD(P)H or Fd (25), various CBB metabolic intermediates (reviewed in ref. 26), calcium signaling (15, 27), phosphorylation of CEF-related proteins (27), and the reactive oxygen species H<sub>2</sub>O<sub>2</sub> (26–29).

## Significance

Cyclic electron flow around photosystem I (CEF) is critical for balancing the energy budget of photosynthesis, but its regulation is not well understood. Our results provide evidence that hydrogen peroxide, which is produced as a result of imbalances in chloroplast redox state, acts as a signaling agent to activate CEF in higher plants in vivo.

Author contributions: D.D.S., A.K.L., M.S.-C., J.E.F., V.G.M., and D.M.K. designed research; D.D.S., A.K.L., M.S.-C., and J.E.F. performed research; D.D.S., A.K.L., M.S.-C., and J.E.F. analyzed data; and D.D.S., A.K.L., and D.M.K. wrote the paper.

The authors declare no conflict of interest.

This article is a PNAS Direct Submission.

Freely available online through the PNAS open access option.

<sup>1</sup>Present address: Department of Biology, Portland Community College, Portland, OR 97219.

<sup>2</sup>To whom correspondence should be addressed. Email: kramerdb@msu.edu.

This article contains supporting information online at [www.pnas.org/lookup/suppl/doi:10.1073/pnas.1418223112/-DCSupplemental](http://www.pnas.org/lookup/suppl/doi:10.1073/pnas.1418223112/-DCSupplemental).

One possibility is that CEF may be at least partly regulated by  $H_2O_2$  (26), which is produced by the light reactions of photosynthesis and already known to regulate other cellular processes such as plant growth, development, and defense (30–32). Based on *in vitro* studies, it was previously proposed that  $H_2O_2$  could activate CEF or chlororespiration by modifying the NDH complex (27). It has also been shown that  $H_2O_2$  can increase the expression of the NDH complex (29) and may further affect the accumulation of photosynthetic metabolites, indirectly activating CEF (26). Consistent with this possibility,  $H_2O_2$  is a well-documented signaling molecule (33), possibly through its ability to oxidize thiols (34, 35). Furthermore,  $H_2O_2$  is expected to be produced under many conditions that initiate CEF [e.g., under a deficit of ATP, when electrons should accumulate in the PSI acceptor pools, leading to superoxide production that can be converted to  $H_2O_2$  by superoxide dismutase (36)].

This study aims to test the hypothesis that CEF can be initiated *in vivo* by  $H_2O_2$  using a combination of *in vivo* spectroscopy and genetic modifications to selectively and rapidly initiate  $H_2O_2$  production in the chloroplast.

## Results

**$H_2O_2$  Accumulation in the High-CEF Mutant *hcef1*.** The *Arabidopsis* mutant *hcef1* (37), which is deficient in chloroplastic fructose 1,6-bisphosphatase (FBPase) activity and displays constitutively high CEF rates, was tested for increased  $H_2O_2$  accumulation. When measured by the Amplex Red assay (Fig. 1) *hcef1* showed three times as much  $H_2O_2$  as the wild-type Columbia-0 (Col-0) ( $2.99 \pm 0.17$  and  $1.00 \pm 0.13$ , respectively,  $n = 3$ ,  $P > 0.001$ , Student's *t* test). This result was confirmed by staining leaves with 3,3'-diaminobenzidine (DAB), showing that *hcef1* (Fig. 1, *Inset B*) showed qualitatively increased levels of  $H_2O_2$  compared with Col-0 (Fig. 1, *Inset A*). These results indicate that the loss of FBPase in *hcef1* led to increased  $H_2O_2$  accumulation, probably resulting from a buildup of reducing intermediates of photosynthetic electron transfer (37), and are consistent with a functional connection between  $H_2O_2$  and CEF activation.

**Effects of  $H_2O_2$  Production by Plants Expressing Glycolate Oxidase in Chloroplast.** We next tested whether CEF is activated when intracellular  $H_2O_2$  production is rapidly induced. To achieve this, we compared photosynthetic properties of Col-0 and transgenic *Arabidopsis* plants that express glycolate oxidase (GO) targeted to the chloroplast (38). These "GO" plants produce  $H_2O_2$  in the chloroplast by the oxidation of glycolate upon activation of photorespiration, and are thus useful tools for studying changes in photosynthetic activities induced by the metabolic generation of  $H_2O_2$  in the chloroplast. We focus mainly on the GO5 line because of its relatively high and robust  $H_2O_2$  production rates (38, 39) (Fig. S1), but we obtained similar results with other lines (discussed below).

GO expression had measurable effects on several photosynthetic parameters (Fig. S2). PSII photochemical efficiency ( $\phi_{II}$ ) (Fig. S2A) and LEF (Fig. S2B) (calculated by variable chlorophyll fluorescence yield) (40, 41) saturated more rapidly with increasing light intensity in GO5 compared with Col-0, leading to a lower LEF, particularly at intensities above  $200 \mu\text{mol photons}\cdot\text{m}^{-2}\cdot\text{s}^{-1}$ . GO5 showed stronger activation of the photo-protective  $q_E$  response (Fig. S2C), likely indicating an increase in light-induced *pmf* and lumen acidification. A substantial (about twofold) increase in *pmf* in GO5 was confirmed by the extent of the rapid light–dark change in the electrochromic shift (ECS<sub>t</sub>), which is proportional the light-induced *pmf* (42–44, *Methods*). Increased *pmf* occurred in GO5 despite a lower LEF, suggesting that either proton influx was increased above that supported by LEF alone or that proton efflux was slowed.

The conductivity of the thylakoid to protons ( $g_{H^+}$ ), which primarily reflects the activity of the ATP synthase, was estimated

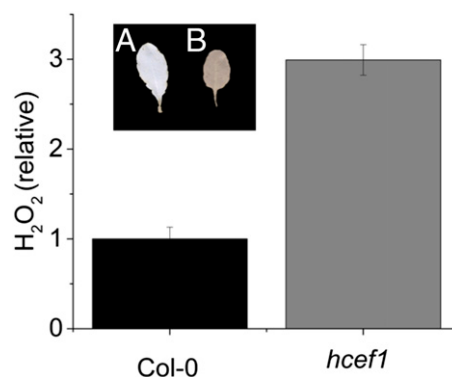


**Fig. 1.** The *hcef1* mutant shows elevated  $H_2O_2$  accumulation. Leaf  $H_2O_2$  content was determined using the Amplex Red assays and expressed as resorufin fluorescence against a standard curve. Results were normalized to the average Col-0  $H_2O_2$  content. Data are presented on a per-leaf area basis. Mean  $\pm$  SD,  $n = 3$ . (*Inset*) Qualitative  $H_2O_2$  accumulation measured by DAB staining of representative leaves of Col-0 (A) and *hcef1* (B). Both assays were performed on leaves from fully mature rosettes as described in Livingston et al. (37).

by the decay kinetics of the electrochromic shift (ECS) signal (43, 45). In GO5,  $g_{H^+}$  was  $\sim 30\%$  lower than in Col-0 (Fig. S2E), implying that, although the ATP synthase activity was somewhat decreased in the mutant, it could not by itself explain the large increase in light-induced *pmf*, suggesting that CEF contributes substantially to *pmf* in GO5 (see discussion in refs. 37 and 46). This conclusion was supported by a statistically significant [analysis of covariance (ANCOVA)  $P < 0.05$ ,  $n = 3$ ] increase of about  $36\%$  in light-driven *pmf*, estimated by ECS<sub>t</sub> as a function of *pmf*<sub>LEF</sub> (Fig. S2F), a parameter that estimates *pmf* generated by LEF alone (44, 47), implying that CEF was activated in GO5.

Increased CEF in GO5 was further indicated by a complementary approach comparing estimated light-driven proton flux ( $v_{H^+}$ ) as a function of LEF (47, 48). As shown in Fig. 2A, the slope of  $v_{H^+}$  as a function of LEF was increased in GO5 in comparison with Col-0 by  $\sim 47.6\%$  (Fig. 2A, ANCOVA  $P < 0.05$ ,  $n = 3$ ). The increase in CEF was eliminated by infiltration of  $100 \mu\text{M}$  methyl viologen, which blocks CEF by shunting electrons from PSI to  $O_2$  (37) (Fig. S3). The increase in relative CEF (calculated by the parameter  $\Delta v_{H^+} / v_{H^+LEF}$ , see Eq. 3, *Methods*) was not caused simply by decreasing LEF because CEF is slow in wild type under nonstressed conditions (see refs. 37 and 46 and Fig. S3). Instead, assuming a similar ratio of proton translocation for electron flux, CEF was observed to increase in GO5 in absolute terms from minimal activation in the control (as previously reported in ref. 37) to  $\sim 24 \mu\text{mol electrons}\cdot\text{m}^{-2}\cdot\text{s}^{-1}$  when LEF was  $50 \mu\text{mol electrons}\cdot\text{m}^{-2}\cdot\text{s}^{-1}$ . Analyzing the ECS and fluorescence data described above (and in *Methods*, Eq. 3), we estimated that  $v_{H^+}$  relative to LEF was increased by about  $50\%$  in GO5 over Col-0, indicating an increase in CEF activation in the mutant (Fig. 2) (see refs. 37 and 46). The difference in the apparent extents of CEF activation (about  $36\%$  versus about  $50\%$ ) may be ascribed to differences in proton to electron stoichiometries for CEF versus LEF or to ambiguities in quantification of the proton and electron fluxes. Moreover, as shown in Figs. S3–S5, the qualitative increase in  $H_2O_2$  content of GO5, GO16, and GO20 and estimates of increased CEF indicate a positive relationship between the extent of  $H_2O_2$  production in multiple GO lines with differing levels of GO activity (38).

Finally, in an independent assessment of CEF induction, we observed a strong increase in GO5 compared with Col-0 of the postillumination chlorophyll fluorescence rise (Fig. S6), which is attributed to CEF-related reduction of the plastoquinone pool in the dark through the NDH complex (9, 49, 50).

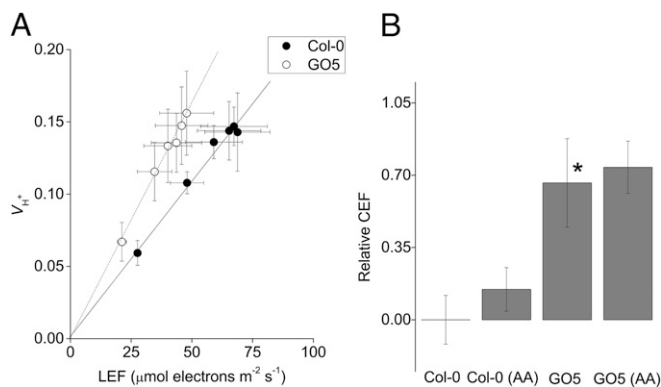


**Fig. 2.** GO5 shows increased CEF relative to Col-0. (A) Light-driven proton flux ( $v_{H^+}$ ) plotted against LEF in attached Col-0 (●) and GO5 (○) leaves. (B) Calculated relative CEF contributions from intact leaves and leaves infiltrated with 20  $\mu\text{M}$  antimycin A (AA). Mean  $\pm$  (A) SD ( $n = 3$ ) or (B) SEM ( $n \geq 3$ ). Asterisk indicates statistical significance from Col-0; no significant differences were seen between water and AA within genotype.

Together, these results strongly imply that introduction of GO in chloroplasts activated CEF. However, in the GO plants glyoxylate, produced by the glycolate oxidase in the chloroplasts, also accumulates and may induce CEF. To test this possibility we measured CEF in GO5 plants also coexpressing malate synthase targeted to the chloroplast (GOMS1 and GOMS14 lines), which can further convert glyoxylate to malate (38). We do not expect large effects of increased malate production because it is already produced in the chloroplast, readily exported through the malate shunt, and subsequently oxidized by the mitochondria. We observed qualitatively similar photosynthetic effects of GO5 and GOMS14 (Fig. S7), indicating that the production of  $\text{H}_2\text{O}_2$  rather than glyoxylate is the likely inducer of CEF (Fig. S7).

The observed increase in CEF was insensitive to infiltration with 20  $\mu\text{M}$  antimycin A (Fig. 2B, ANCOVA,  $P > 0.05$ ,  $n = 3$ ), well above the observed  $K_i$  for inhibition of the antimycin A-sensitive pathway of CEF (51). These results imply that NDH, rather than the PGR5/PGRL1 pathway, is the predominant route for elevated CEF in GO5, and are also in accord with the observed increased postillumination rise (Fig. S6).

Interestingly, when expressed on a chlorophyll basis, the NDH content of GO5 was higher in GO5 than in wild type (Fig. S8), consistent with previous results indicating the accumulation of NDH in response to  $\text{H}_2\text{O}_2$  (29). These results indicate that  $\text{H}_2\text{O}_2$  likely has effects on both short-term activation of NDH and longer-term effects on its expression levels.

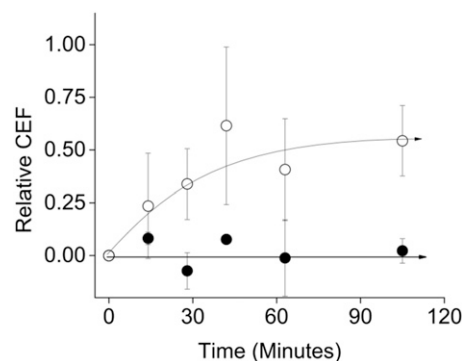
#### Kinetics of CEF Induction upon Activation of $\text{H}_2\text{O}_2$ Production in GO5.

Fig. 3 shows the kinetics of induction of CEF in the GO5 plants upon rapid initiation of  $\text{H}_2\text{O}_2$  production. GO5 plants were initially grown under high (3,000 ppm)  $\text{CO}_2$  conditions to minimize photorespiration (52, 53), thereby preventing the production of  $\text{H}_2\text{O}_2$  by GO (38, 39). Photosynthetic parameters were measured in intact leaves under 2,000 ppm  $\text{CO}_2$  and then rapidly switched to ambient air (about 400 ppm  $\text{CO}_2$ ) at time 0 to initiate  $\text{H}_2\text{O}_2$  production. Steady-state fluorescence and ECS measurements were made every 14 min and analyzed as in Fig. 24 to estimate changes in CEF. Increased CEF appeared with a half time of about 20 min, reaching an apparent maximum relative CEF of 0.62, or a 62% increase in  $v_{H^+}/\text{LEF}$ , in 42 min ( $\Delta v_{H^+}/v_{H^+}^{\text{LEF}}$ , see Eq. 3, Methods). No increase in CEF was seen in similarly treated Col-0 leaves (Fig. 3).

**Induction of CEF by Infiltration of Leaves with  $\text{H}_2\text{O}_2$ .** Fig. 4 shows the effects of infiltration of aqueous solutions of  $\text{H}_2\text{O}_2$  into Col-0

leaves on induction of CEF, measured as in Fig. 3. As we previously described, there was very little contribution from CEF in Col-0 plants under nonstressed control conditions, implying that under these conditions other mechanisms (e.g., malate valve or the Mehler reaction) are sufficient to balance ATP and NADPH requirements (47, 54). Infiltration of leaves with as low as 300  $\mu\text{M}$  (0.001%)  $\text{H}_2\text{O}_2$  led to induction of significant CEF rates in vivo (Fig. 4). The observed  $\text{H}_2\text{O}_2$ -induced increase in CEF depended on the concentration of  $\text{H}_2\text{O}_2$  in the infiltrate, with an apparent half-saturation concentration of about 3 mM. Infiltration of Col-0 with 300  $\mu\text{M}$ , 3 mM, and 30 mM  $\text{H}_2\text{O}_2$  increased the CEF to 21, 42, and 68% compared with LEF over the water-treated controls. Infiltration with higher concentrations of  $\text{H}_2\text{O}_2$  or over longer time periods led to strong loss of photosynthetic activity; these conditions were therefore excluded from this study. Infiltration of  $\text{H}_2\text{O}_2$  into *pgr5* (6), which lacks the antimycin A-sensitive PGR5-dependent CEF pathway, resulted in activation of CEF at Col-0 levels (65%). In contrast,  $\text{H}_2\text{O}_2$  infiltration of *crr2-2*, which is deficient in NDH (10, 55), resulted in very low levels of CEF (5%) (Fig. 4). These results support our conclusion that the  $\text{H}_2\text{O}_2$ -induced CEF occurs predominantly through NDH rather than PGR5/PGRL1.

We also tested for effects of  $\text{H}_2\text{O}_2$  on the postillumination chlorophyll fluorescence rise signal (Fig. 5). In this case, we found it necessary to modify the assay procedure to obtain more reproducible results. The fluorescence rise depends on the presence of both active PQ reductase and sufficiently reduced NADPH and/or Fd pools. In the presence of  $\text{H}_2\text{O}_2$  it is likely that NADPH will be oxidized in the dark by monodehydroascorbate reductase and dehydroascorbate reductase (36, 56), thus inhibiting the CEF-dependent fluorescence rise. We circumvented this problem by flushing with  $\text{N}_2$  immediately before and during the duration of the experiment, thus ensuring that the NADPH pool is strongly reduced. Under these conditions the fluorescence rise was much stronger and more rapid even in the control leaves (compare Fig. 5 and Fig. S6). In fact, the rise in fluorescence, particularly after infiltration with 30 mM  $\text{H}_2\text{O}_2$ , was sufficiently rapid as to overlap with the oxidation that occurs after switching off the actinic light. Therefore, to distinguish the CEF-related reduction, we applied a series of two far-red light pulses to transiently oxidize the PQ pool (Fig. 5, Inset), after which we observed its rereduction, presumably through the CEF-related plastoquinone reductase. The postfar-red fluorescence rise was substantially larger and more rapid after exposure to  $\text{H}_2\text{O}_2$ . In fact,  $\text{H}_2\text{O}_2$ -treated leaves showed higher fluorescence yield even



**Fig. 3.** Induction kinetics of CEF activation upon initiation of intracellular  $\text{H}_2\text{O}_2$  production. The activation time course for CEF in Col-0 (●) and GO5 (○) were determined upon switching atmosphere from 2,000 ppm  $\text{CO}_2$  to 400 ppm  $\text{CO}_2$  at time 0 to activate photorespiration. Relative CEF was determined as described in Fig. 1. Reported values are the mean of three biological trials  $\pm$  SEM.



in the dark period at the beginning of the experiment, suggesting that the plastoquinone pool was reduced even before illumination. These results support the hypothesis that the PQ reductase was more activated after exposure to H<sub>2</sub>O<sub>2</sub>.

## Discussion

**CEF Is Induced by H<sub>2</sub>O<sub>2</sub> Production in Vivo.** Past work has shown that mutants in higher plants that accumulate highly reducing stromal redox components also induce elevated CEF, for example mutants deficient in FBPase (i.e., *hcefl*), aldolase, and glyceraldehyde-3-phosphate dehydrogenase (26, 37, 50). Similarly, certain environmental conditions (e.g., drought stress) lead to both increased H<sub>2</sub>O<sub>2</sub> and elevated CEF (57, 58). In contrast, simply decreasing the rate of photosynthesis without increased levels of H<sub>2</sub>O<sub>2</sub> does not seem to induce CEF (26, 59).

These observations suggest a possible regulatory link between H<sub>2</sub>O<sub>2</sub> production and the activation of CEF. To test this possibility, we used transgenic GO plants, which express a chloroplast-targeted glycolate oxidase, and conditionally produce H<sub>2</sub>O<sub>2</sub> under photorespiratory conditions. Activation of H<sub>2</sub>O<sub>2</sub> production in GO5 had strong effects on photosynthesis, decreasing LEF, increasing thylakoid *pmf*, and activating *q<sub>E</sub>* (Fig. S2). Most strikingly, elevated H<sub>2</sub>O<sub>2</sub> production led to strong activation of CEF (Fig. 2 and Fig. S2F). CEF was similarly induced by infiltration of leaves with H<sub>2</sub>O<sub>2</sub> (Fig. 4) but was unaffected by expressing malate synthase, which metabolizes glyoxylate produced by GO (38). This implies that the effects were primarily caused by H<sub>2</sub>O<sub>2</sub> and not by GO-induced changes in metabolic intermediates. Experiments with the inhibitor antimycin A and mutants lacking NDH or PGR5 indicate that the CEF induced in GO5 or upon H<sub>2</sub>O<sub>2</sub> infiltration occurs mainly, if not exclusively, through the NDH pathway (Fig. 2B and Fig. S6).

The activation of CEF after the onset of H<sub>2</sub>O<sub>2</sub> production was likely too rapid (halftime of about 20 min, Fig. 3), to involve de novo protein synthesis, which is expected to be considerably slower (60, 61), suggesting that short-term H<sub>2</sub>O<sub>2</sub> production can activate preexisting CEF machinery, consistent with a mechanism for rapid activation of CEF to meet fluctuating ATP demands, as proposed earlier (27). In addition, H<sub>2</sub>O<sub>2</sub> was shown in previous studies (29) as well as in this work (Fig. S8) to induce higher levels of NDH proteins, suggesting a dual mode of action both at the enzyme and expression levels.

**H<sub>2</sub>O<sub>2</sub> Activates the Antimycin A-Insensitive Pathway.** H<sub>2</sub>O<sub>2</sub>-induced CEF was insensitive to antimycin A (Fig. 2B). In addition, activation of CEF by infiltration with H<sub>2</sub>O<sub>2</sub> was inhibited in the NDH-deficient *crr2-2* mutant (Fig. 4), whereas the mutant deficient in

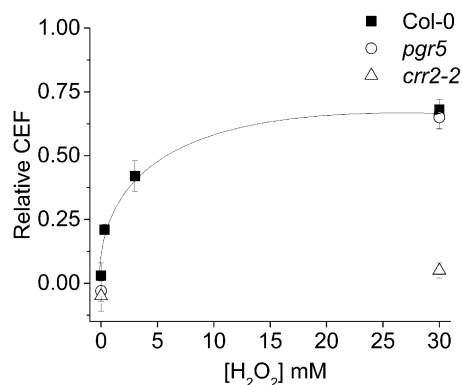


**Fig. 4.** Activation of CEF in wild type leaves by foliar infiltration with solutions of H<sub>2</sub>O<sub>2</sub>. Changes in relative CEF levels in Col-0 (■), *pgr5* (○), and *crr2-2* (△) leaves after incubation with increasing concentrations of H<sub>2</sub>O<sub>2</sub>. Mean ± SD (*n* = 3).

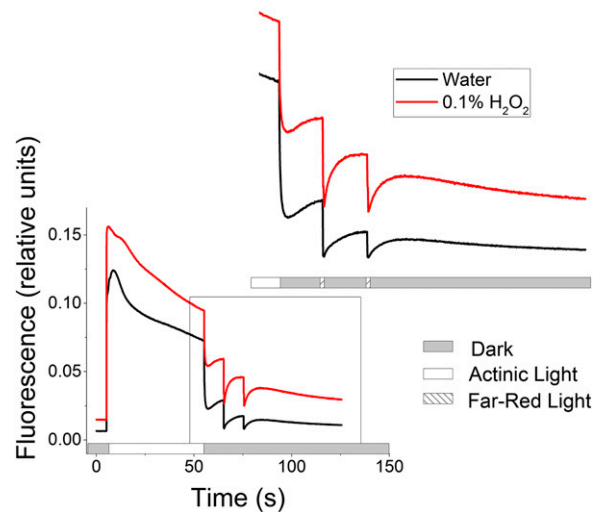


**Fig. 5.** Increased dark reduction of the PQ/PQH<sub>2</sub> pool in leaves infiltrated with 30 mM H<sub>2</sub>O<sub>2</sub> for 3 h. Transient chlorophyll fluorescence rise in the dark, and after far-red pulses (730 nm), after actinic illumination with 150 μmol photons·m<sup>-2</sup>·s<sup>-1</sup> under 100% N<sub>2</sub> gas. Water (black) and 30 mM H<sub>2</sub>O<sub>2</sub> (red) representative data of two independent experiments.

PGR5 was activated to Col-0 levels. These results imply that H<sub>2</sub>O<sub>2</sub>-induced CEF does not involve the PGR5/PGRL1 pathway (4, 6, 7) but favors the involvement of the chloroplast NDH complex, as previously shown in *hcefl* (37). Consistent with this view, accumulation and phosphorylation of the NDH complex has been associated with increased activity in the presence of oxidative stress (27, 29), and its activation results in increased postillumination fluorescence rise, which was increased in the GO5 mutant (Fig. S6).

**A Regulatory Role for H<sub>2</sub>O<sub>2</sub> in Activation of CEF?** Regulation of CEF likely involves distinct processes in different species (e.g., green algal and plant chloroplasts use different plastoquinone reductases) (14, 62). Recent work by Takahashi et al. (19) and Lucker and Kramer (22) suggests that CEF in *Chlamydomonas* is regulated by changes in stromal redox status that result from imbalances in the supply and demand for NADPH relative to ATP. However, it is not yet clear which redox components are involved. In the case of higher plants, a survey of CEF activation results from a range of mutant lines led Livingston et al. (26) to argue against any simplistic model where a single redox carrier could serve as the regulator.

Based on the results presented here, we propose a hypothetical model in which H<sub>2</sub>O<sub>2</sub> production can regulate the activation of CEF in higher-plant chloroplasts. A deficit of ATP in the stroma should prevent the turnover of assimilatory reactions and cause a buildup of reductants (NADPH, Fd, and PSI acceptors), leading to generation of superoxide and H<sub>2</sub>O<sub>2</sub>. When the rate of H<sub>2</sub>O<sub>2</sub> production exceeds that of its detoxification by the water-water cycle (36) it may accumulate and interact with one or more proteins regulating the activity of the antimycin A-insensitive pathway of CEF, possibly via a signal cascade, leading to the increased expression and phosphorylation of NDH as suggested by refs. 27 and 29, or by inactivating CBB enzymes, leading to secondary redox or metabolic signaling.

## Methods

**Plant Material and Growth Conditions.** All plants, Col-0, GO plants [expressing glycolate oxidase targeted to the chloroplast (38)], and *hcefl* (37) were grown in soil under growth chamber conditions with 16 h light of white light (~80 μmol photons·m<sup>-2</sup>·s<sup>-1</sup>) and 8 h of darkness photoperiod and a 22 °C/18 °C (day/night) cycle. Where noted, plants were grown under the

same conditions but at high (3,000 ppm) CO<sub>2</sub> to prevent the production of H<sub>2</sub>O<sub>2</sub> in GO through the photorespiratory pathway.

**In Vivo Spectroscopic Assays.** Under ambient CO<sub>2</sub> conditions, the GO plants present with a slightly smaller, pale, and patchy leaf phenotype; however, the chlorotic phenotype disappeared at maturity. Therefore, all spectroscopic measurements were made using intact fully expanded leaves in 25- to 30-d-old plants just before bolting. To fully induce differential H<sub>2</sub>O<sub>2</sub> production, GO5 and all controls were preilluminated for 1 h at 350 μmol photons·m<sup>-2</sup>·s<sup>-1</sup>. Plants were then dark adapted for 10 min before analysis. Actinic light intensities ranged between 50–600 μmol photons·m<sup>-2</sup>·s<sup>-1</sup>. Chlorophyll a fluorescence yield changes and light-induced absorbance changes were measured using on a laboratory-built spectrophotometer/fluorimeter (63) using the techniques described in ref. 37. Saturation pulse chlorophyll a fluorescence yield parameters (F<sub>0</sub>, F<sub>M</sub>, F<sub>S</sub>, F<sub>M</sub><sup>′</sup>, F<sub>M</sub><sup>′′</sup>) were recorded as described (40, 44, 47, 64), using 1-s saturation pulses of ~10,000 μmol photons·m<sup>-2</sup>·s<sup>-1</sup>. These measurements were used to estimate the yield of PSII (φ<sub>II</sub>), LEF, and the rapidly reversible component of nonphotochemical quenching, q<sub>E</sub> (41, 65). LEF was calculated as

$$\phi_{II} * i * 0.4, \quad [1]$$

where *i* is the actinic light intensity. Leaf absorptivity of the GO plants did not differ significantly from Col-0 (*P* = 0.78, *n* = 3).

The ECS measurements were normalized for variations in leaf thickness and pigmentation by the extent of the rapid-rise single-turnover flash-induced ECS (37, 47). The ECS<sub>t</sub> and τ<sub>ECS</sub> parameters were taken from a first-order exponential decay fit to ECS dark interval relaxation kinetics as described in ref. 44. The *pmf*<sub>LEF</sub> parameter, estimating relative extents of *pmf* attributable to LEF, was calculated as

$$pmf_{LEF} = LEF/g_{H^+}. \quad [2]$$

Postillumination transient chlorophyll fluorescence transients in Fig. S6 were measured as described in ref. 50. Transients in Fig. 5 were obtained under N<sub>2</sub> gas throughout the experiment. Leaves were illuminated for 40 s with 150 μmol photons·m<sup>-2</sup>·s<sup>-1</sup>, followed by a 10-s dark interval. The plastoquinone pool was then oxidized by two 200-ms flashes of 730-nm light 10 s apart.

**Infiltration of Leaves with H<sub>2</sub>O<sub>2</sub>, Methyl Viologen, and Antimycin A.** To determine the effects of H<sub>2</sub>O<sub>2</sub> on CEF, Col-0 leaves were detached and soaked in distilled water or solutions of various concentrations of H<sub>2</sub>O<sub>2</sub> for 120 min between two layers of tissue paper (Kimwipe) under ambient laboratory lighting (~20 μmol photons·m<sup>-2</sup>·s<sup>-1</sup>). Excess liquid was removed from the leaf material before analysis by gentle blotting with a fresh Kimwipe.

Where indicated, leaves were incubated as above for 60 min at low light (5~15 μmol photons·m<sup>-2</sup>·s<sup>-1</sup>) in either distilled water or a solution of 100 μM methyl viologen in water (37). Infiltration with 20 μM antimycin A was carried out in darkness for 3 h. Successful antimycin A infiltration was confirmed by loss of the transient fluorescence quenching during photosynthetic induction as previously described (66).

**Manipulation of Gas Concentrations.** Humidified ambient air was supplied to the underside of the leaf unless indicated otherwise. Fluctuating CO<sub>2</sub> concentrations were obtained using a gas mixer (LiCor 6400) connected to a CO<sub>2</sub> gas cylinder (Airgas). Where indicated, N<sub>2</sub> gas (Airgas) was supplied with low flow to the underside of the leaf.

**Measurement of H<sub>2</sub>O<sub>2</sub> Production in Leaves.** Hydrogen peroxide was detected by resorufin (modified from ref. 67). Leaf discs of the same size were rapidly frozen and ground in liquid nitrogen and extracted in 50 mM potassium phosphate buffer (pH 7.5). Extracts were incubated in a reaction buffer containing 10 U·mL<sup>-1</sup> horseradish peroxidase (Sigma) and 5 μM Amplex Red (Invitrogen) for 30 min in the dark. Peroxide concentration of the sample was estimated by comparison with a standard curve, and relative values were calculated by normalizing to the Col-0 average.

Visualization of H<sub>2</sub>O<sub>2</sub> production was determined using the DAB staining technique modified from previous work (38). Fully expanded leaves were wrapped in a Kimwipe tissue paper, soaked with 1 mg·mL<sup>-1</sup> DAB in distilled water, and incubated for 1 h in the dark to allow for uptake. The leaves were placed on top of the DAB-soaked tissue paper, and illuminated with ~90 μmol·m<sup>-2</sup>·s<sup>-1</sup> of light for 50 min. Natural leaf pigmentation was then removed from the leaf by boiling in 95% ethanol. For GO5 plants, leaf age was as describe above for spectroscopic assays. For *hcef1*, leaf age was as described for spectroscopic measurements in Livingston et al. (37).

**Protein Extraction and Western Blot.** Total leaf protein was extracted from fully mature rosettes as described in ref. 37. Proteins were separated by SDS/PAGE on a 16% polyacrylamide Tris-Tricine gel. Protein was transferred to a PVDF membrane and probed with an anti-NDH-18, a gift from T. Shikanai, Kyoto University, Kyoto, and secondary anti-rabbit conjugated to alkaline phosphatase and developed colorimetrically.

**Measurements of CEF.** LEF, with no contributions from CEF, should produce a constant ratio of proton flux to electron transfer through PSII of 3 H<sup>+</sup>/e<sup>-</sup> (54), which in our measurements should result in a constant, linear slope of v<sub>H<sup>+</sup></sub> plotted against LEF. The relative rates of CEF can then be estimated by the increase in the slope of v<sub>H<sup>+</sup></sub> versus LEF above the baseline slope for LEF alone (26). Relative CEF, which is proportional to the v<sub>H<sup>+</sup></sub> rate attributable to CEF when the H<sup>+</sup>/e<sup>-</sup> ratio is the same for CEF as for LEF, was expressed as a fraction increase over the v<sub>H<sup>+</sup></sub> attributable to LEF (Δv<sub>H<sup>+</sup></sub>/v<sub>H<sup>+</sup></sub>LEF) and was calculated by

$$\text{Relative CEF} \propto (m_{(CEF+LEF)} - m_{(LEF)})/m_{(LEF)}, \quad [3]$$

where *m*<sub>(CEF+LEF)</sub> and *m*<sub>(LEF)</sub> are the slopes of best fit lines for v<sub>H<sup>+</sup></sub> plotted against LEF in treated or mutant leaves and untreated or Col-0 leaves, respectively. Control experiments were performed after infiltration with 100 μM methyl viologen to eliminate CEF and were used as a baseline indicating slopes with no CEF contributions, as described previously (37, 47).

**Statistical Analysis.** Descriptive statistics and figures were generated using Origin 9.0 software (Microcal Software), and statistical analyses were performed using MATLAB R2012a (The MathWorks, Inc.) or Microsoft Excel. All *P* values less than 0.05 were considered statistically significant and are noted within the text.

**ACKNOWLEDGMENTS.** We thank Drs. Nicholas Fisher, Atsuko Kanazawa, and Jeffrey Cruz for helpful discussions, and Dr. Toshiharu Shikanai for his kind donation of *pgf5* and *crr2-2* seed and for the generous donation of the anti-NDH-18 antibody. The work was funded by Grants DE-FG02-11ER16220 (supporting the biochemical and biophysical analyses by D.D.S., A.K.L., M.S.-C., and D.M.K.) and DE-FG02-04ER15559 (supporting the proteomics work by J.E.F.) from Division of Chemical Sciences, Geosciences, and Biosciences, Office of Basic Energy Sciences of the US Department of Energy. The development of the GO mutants was funded by the Deutsche Forschungsgemeinschaft through Grant MA2379/11-1 (to V.G.M.).

- Müller P, Li XP, Niyogi KK (2001) Non-photochemical quenching. A response to excess light energy. *Plant Physiol* 125(4):1558–1566.
- Eberhard S, Finazzi G, Wollman F-A (2008) The dynamics of photosynthesis. *Annu Rev Genet* 42:463–515.
- Kramer DM, Evans JR (2011) The importance of energy balance in improving photosynthetic productivity. *Plant Physiol* 155(1):70–78.
- Bendall DS, Manasse RS (1995) Cyclic photophosphorylation and electron transport. *Biochim Biophys Acta* 8:23–38.
- Munekage Y, Hashimoto M, Miyake C (2004) Cyclic electron flow around photosystem I is essential for photosynthesis. *Nature* 429:579–582.
- Munekage Y, et al. (2002) PGR5 is involved in cyclic electron flow around photosystem I and is essential for photoprotection in Arabidopsis. *Cell* 110(3):361–371.
- Hertle AP, et al. (2013) PGR1 is the elusive ferredoxin-plastoquinone reductase in photosynthetic cyclic electron flow. *Mol Cell* 49(3):511–523.
- Sazanov LA, Burrows PA, Nixon PJ (1998) The plastid ndh genes code for an NADH-specific dehydrogenase: Isolation of a complex I analogue from pea thylakoid membranes. *Proc Natl Acad Sci USA* 95(3):1319–1324.
- Burrows PA, Sazanov LA, Svab Z, Maliga P, Nixon PJ (1998) Identification of a functional respiratory complex in chloroplasts through analysis of tobacco mutants containing disrupted plastid ndh genes. *EMBO J* 17(4):868–876.
- Suorsa M, Sirpiö S, Aro E-M (2009) Towards characterization of the chloroplast NAD(P)H dehydrogenase complex. *Mol Plant* 2(6):1127–1140.
- Yamamoto H, Peng L, Fukao Y, Shikanai T (2011) An Src homology 3 domain-like fold protein forms a ferredoxin binding site for the chloroplast NADH dehydrogenase-like complex in Arabidopsis. *Plant Cell* 23(4):1480–1493.
- Hasan SS, Yamashita E, Baniulis D, Cramer WA (2013) Quinone-dependent proton transfer pathways in the photosynthetic cytochrome b<sub>6</sub>f complex. *Proc Natl Acad Sci USA* 110(11):4297–4302.
- Zhang H, Whitelegge JP, Cramer WA (2001) Ferredoxin:NADP+ oxidoreductase is a subunit of the chloroplast cytochrome b<sub>6</sub>f complex. *J Biol Chem* 276(41):38159–38165.
- Iwai M, et al. (2010) Isolation of the elusive supercomplex that drives cyclic electron flow in photosynthesis. *Nature* 464(7292):1210–1213.
- Terashima M, et al. (2012) Calcium-dependent regulation of cyclic photosynthetic electron transfer by a CAS, ANR1, and PGR1 complex. *Proc Natl Acad Sci USA* 109(43):17717–17722.

16. Alric J (2014) Redox and ATP control of photosynthetic cyclic electron flow in *Chlamydomonas reinhardtii*: (II) involvement of the PGR5-PGRL1 pathway under anaerobic conditions. *Biochim Biophys Acta* 1837(6):825–834.
17. Johnson X, et al. (2014) Proton gradient regulation 5-mediated cyclic electron flow under ATP- or redox-limited conditions: A study of  $\Delta$ ATPase pgr5 and  $\Delta$ rbcL pgr5 mutants in the green alga *Chlamydomonas reinhardtii*. *Plant Physiol* 165(1):438–452.
18. Finazzi G, et al. (2002) Involvement of state transitions in the switch between linear and cyclic electron flow in *Chlamydomonas reinhardtii*. *EMBO Rep* 3(3):280–285.
19. Takahashi H, Clowse S, Wollman F-A, Vallon O, Rappaport F (2013) Cyclic electron flow is redox-controlled but independent of state transition. *Nat Commun* 4:1954.
20. Cardol P, et al. (2009) Impaired respiration discloses the physiological significance of state transitions in *Chlamydomonas*. *Proc Natl Acad Sci USA* 106(37):15979–15984.
21. Havaux M, Rumeau D, Ducruet J-M (2005) Probing the FQR and NDH activities involved in cyclic electron transport around Photosystem I by the 'afterglow' luminescence. *Biochim Biophys Acta* 1709(3):203–213.
22. Lucker B, Kramer DM (2013) Regulation of cyclic electron flow in *Chlamydomonas reinhardtii* under fluctuating carbon availability. *Photosynth Res* 117(1-3):449–459.
23. Joliot P, Joliot A (2006) Cyclic electron flow in C3 plants. *Biochim Biophys Acta* 1757(5-6):362–368.
24. Joliot P, Joliot A (2002) Cyclic electron transfer in plant leaf. *Proc Natl Acad Sci USA* 99(15):10209–10214.
25. Breyton C, Nandha B, Johnson GN, Joliot P, Finazzi G (2006) Redox modulation of cyclic electron flow around photosystem I in C3 plants. *Biochemistry* 45(45):13465–13475.
26. Livingston AK, Kanazawa A, Cruz JA, Kramer DM (2010) Regulation of cyclic electron flow in C<sub>3</sub> plants: Differential effects of limiting photosynthesis at ribulose-1,5-bisphosphate carboxylase/oxygenase and glyceraldehyde-3-phosphate dehydrogenase. *Plant Cell Environ* 33(11):1779–1788.
27. Lascano HR, Casano LM, Martin M, Sabater B (2003) The activity of the chloroplastic Ndh complex is regulated by phosphorylation of the NDH-F subunit. *Plant Physiol* 132(1):256–262.
28. Gambarova NG (2008) Activity of photochemical reactions and accumulation of hydrogen peroxide in chloroplasts under stress conditions. *Russ Agric Sci* 34:149–151.
29. Casano LM, Martin M, Sabater B (2001) Hydrogen peroxide mediates the induction of chloroplastic Ndh complex under photooxidative stress in barley. *Plant Physiol* 125(3):1450–1458.
30. Traverso JA, Pulido A, Rodriguez-García MI, Alcázar JD (2013) Thiol-based redox regulation in sexual plant reproduction: New insights and perspectives. *Front Plant Sci* 4:465.
31. O'Brien JA, Daudi A, Butt VS, Bolwell GP (2012) Reactive oxygen species and their role in plant defence and cell wall metabolism. *Planta* 236(3):765–779.
32. Karpiński S, Szechyńska-Hebda M, Wituszyńska W, Burdialek P (2013) Light acclimation, retrograde signalling, cell death and immune defences in plants. *Plant Cell Environ* 36(4):736–744.
33. Lushchak VI (2011) Adaptive response to oxidative stress: Bacteria, fungi, plants and animals. *Comp Biochem Physiol C Toxicol Pharmacol* 153(2):175–190.
34. Buchanan BB, Balmer J (2005) Redox regulation: A broadening horizon. *Annu Rev Plant Biol* 56:187–220.
35. Hancock J, et al. (2006) Doing the unexpected: Proteins involved in hydrogen peroxide perception. *J Exp Bot* 57(8):1711–1718.
36. Asada K (2006) Production and scavenging of reactive oxygen species in chloroplasts and their functions. *Plant Physiol* 141(2):391–396.
37. Livingston AK, Cruz JA, Kohzuma K, Dhingra A, Kramer DM (2010) An Arabidopsis mutant with high cyclic electron flow around photosystem I (*hcef*) involving the NADPH dehydrogenase complex. *Plant Cell* 22(1):221–233.
38. Fahnstich H, Scarpeci TE, Valle EM, Flügge U-I, Maurino VG (2008) Generation of hydrogen peroxide in chloroplasts of Arabidopsis overexpressing glycolate oxidase as an inducible system to study oxidative stress. *Plant Physiol* 148(2):719–729.
39. Balazadeh S, Jaspert N, Arif M, Mueller-Roeber B, Maurino VG (2012) Expression of ROS-responsive genes and transcription factors after metabolic formation of H<sub>2</sub>O<sub>2</sub> in chloroplasts. *Front Plant Sci* 3:234.
40. Baker NR (2008) Chlorophyll fluorescence: A probe of photosynthesis in vivo. *Annu Rev Plant Biol* 59:89–113.
41. Genty B, Briantais J-M, Baker NR (1989) The relationship between the quantum yield of photosynthetic electron transport and quenching of chlorophyll fluorescence. *Biochim Biophys Acta* 990:87–92.
42. Cruz JA, et al. (2005) Plasticity in light reactions of photosynthesis for energy production and photoprotection. *J Exp Bot* 56(411):395–406.
43. Sacksteder CA, Kramer DM (2000) Dark-interval relaxation kinetics (DIRK) of absorbance changes as a quantitative probe of steady-state electron transfer. *Photosynth Res* 66(1-2):145–158.
44. Baker NR, Harbinson J, Kramer DM (2007) Determining the limitations and regulation of photosynthetic energy transduction in leaves. *Plant Cell Environ* 30(9):1107–1125.
45. Avenson TJ, et al. (2005) Integrating the proton circuit into photosynthesis: Progress and challenges. *Plant Cell Environ* 28:97–109.
46. Avenson TJ, Cruz JA, Kanazawa A, Kramer DM (2005) Regulating the proton budget of higher plant photosynthesis. *Proc Natl Acad Sci USA* 102(27):9709–9713.
47. Avenson TJ, Cruz JA, Kramer DM (2004) Modulation of energy-dependent quenching of excitons in antennae of higher plants. *Proc Natl Acad Sci USA* 101(15):5530–5535.
48. Takizawa K, Cruz JA, Kanazawa A, Kramer DM (2007) The thylakoid proton motive force *in vivo*. Quantitative, non-invasive probes, energetics, and regulatory consequences of light-induced pmf. *Biochim Biophys Acta* 1767(10):1233–1244.
49. Shikanai T, et al. (1998) Directed disruption of the tobacco *ndhB* gene impairs cyclic electron flow around photosystem I. *Proc Natl Acad Sci USA* 95(16):9705–9709.
50. Gotoh E, Matsumoto M, Ogawa K, Kobayashi Y, Tsuyama M (2010) A qualitative analysis of the regulation of cyclic electron flow around photosystem I from the post-illumination chlorophyll fluorescence transient in Arabidopsis: A new platform for the *in vivo* investigation of the chloroplast redox state. *Photosynth Res* 103(2):111–123.
51. Cleland RE, Bendall DS (1992) Photosystem I cyclic electron transport: Measurement of ferredoxin-plastoquinone reductase activity. *Photosynth Res* 34(3):409–418.
52. Brooks A, Farquhar GD (1985) Effect of temperature on the CO<sub>2</sub>/O<sub>2</sub> specificity of ribulose-1,5-bisphosphate carboxylase/oxygenase and the rate of respiration in the light: Estimates from gas-exchange measurements on spinach. *Planta* 165(3):397–406.
53. Sharkey TD (1988) Estimating the rate of photorespiration in leaves. *Physiol Plant* 73:147–152.
54. Sacksteder CA, Kanazawa A, Jacoby ME, Kramer DM (2000) The proton to electron stoichiometry of steady-state photosynthesis in living plants: A proton-pumping Q cycle is continuously engaged. *Proc Natl Acad Sci USA* 97(26):14283–14288.
55. Hashimoto M, Endo T, Peltier G, Tasaka M, Shikanai T (2003) A nucleus-encoded factor, *CR2*, is essential for the expression of chloroplast *ndhB* in Arabidopsis. *Plant J* 36(4):541–549.
56. Asada K (2000) The water-water cycle as alternative photon and electron sinks. *Philos Trans R Soc Lond B Biol Sci* 355(1402):1419–1431.
57. Cruz de Carvalho MH (2008) Drought stress and reactive oxygen species: Production, scavenging and signaling. *Plant Signal Behav* 3(3):156–165.
58. Kohzuma K, et al. (2009) The long-term responses of the photosynthetic proton circuit to drought. *Plant Cell Environ* 32(3):209–219.
59. Badger MR, von Caemmerer S, Ruuska S, Nakano H (2000) Electron flow to oxygen in higher plants and algae: Rates and control of direct photoreduction (Mehler reaction) and rubisco oxygenase. *Philos Trans R Soc Lond B Biol Sci* 355(1402):1433–1446.
60. Ma X, Browse J (2006) Altered rates of protein transport in Arabidopsis mutants deficient in chloroplast membrane unsaturation. *Phytochemistry* 67(15):1629–1636.
61. Conte L, Trumpower BL, Zara V (2011) Bcs1p can rescue a large and productive cytochrome bc1 complex assembly intermediate in the inner membrane of yeast mitochondria. *Biochim Biophys Acta* 1813(1):91–101.
62. Desplats C, et al. (2009) Characterization of Nda2, a plastoquinone-reducing type II NAD(P)H dehydrogenase in *Chlamydomonas* chloroplasts. *J Biol Chem* 284(7):4148–4157.
63. Hall C, et al. (2013) Photosynthetic Measurements with the Idea Spec: An Integrated Diode Emitter Array Spectrophotometer/Fluorometer. *Photosynthesis Research for Food, Fuel and Future*, eds Kuang T, Lu C, Zhang L (Springer, Heidelberg), pp 184–188.
64. Kanazawa A, Kramer DM (2002) *In vivo* modulation of nonphotochemical exciton quenching (NPQ) by regulation of the chloroplast ATP synthase. *Proc Natl Acad Sci USA* 99(20):12789–12794.
65. Edwards GE, Baker NR (1993) Can CO<sub>2</sub> assimilation in maize leaves be predicted accurately from chlorophyll fluorescence analysis? *Photosynth Res* 37(2):89–102.
66. Oxborough K, Horton P (1987) Characterisation of the effects of Antimycin A upon high energy state quenching of chlorophyll fluorescence (qE) in spinach and pea chloroplasts. *Photosynth Res* 12(2):119–127.
67. Mubarakshina MM, et al. (2010) Production and diffusion of chloroplastic H<sub>2</sub>O<sub>2</sub> and its implication to signalling. *J Exp Bot* 61(13):3577–3587.